JOURNAL OF SOLID STATE CHEMISTRY **141,** 168–176 (1998)
ARTICLE NO. SC987940

Synthesis and Properties of Erbium Isopropoxides: Structural Characterization of $Er_5O(OPr^i)_{13}$

G. Westin,*,[1] M. Kritikos,† and M. Wijk*

*Department of Inorganic Chemistry and †Department of Structural Chemistry, Arrhenius Laboratory, Stockholm University, S-106 91 Stockholm, Sweden

Received December 15, 1997; in revised form May 18, 1998; accepted June 24, 1998

We have investigated the synthesis of erbium isopropoxides by dissolution of Er metal in 2-propanol-containing solvents or by metathesis of $ErCl_3$ and $KOPr^i$ in solution, with or without addition of water. Two different erbium isopropoxides could be isolated in pure form: one with a structure that has not been solved (I), which we believe to be a solvated non-oxo isopropoxide, and one oxo isopropoxide, $Er_5O(OPr^i)_{13}$. The latter structure was determined by single-crystal X-ray diffraction; it has orthorhombic space group symmetry *Pbca*, $a = 20.917(6)$ Å, $b = 21.575(6)$ Å, $c = 25.638(6)$ Å, with $Z = 8$. The final R value was 0.0748 ($R_w = 0.1158$). The oxo isopropoxide molecules contain the well-known M_5O fragment, which has the configuration of a square pyramid with the oxo-oxygen atom slightly above the basal plane. The compounds have been characterized by FT-IR and UV–vis spectroscopy, differential scanning calorimetry, and their solubilities and chemical reactivities. FT-IR studies revealed that both alkoxides largely retained the molecular structure when dissolved in toluene–2-propanol (2:1) or hexane. The stability of $Er_5O(OPr^i)_{13}$ in the absence of water is rather high, whereas I is more labile. © 1998 Academic Press

1. INTRODUCTION

Alkoxides are the most important precursors in the organic sol–gel technique (1), and knowledge about their structures is important for understanding the sol–gel process itself and for increasing the possibility of tailoring the products. An area that has recently received considerable interest is the sol–gel processing of Nd^{3+}- and Er^{3+}-doped glasses as bulk and wave guide materials (2, 3). Doping with Ln^{3+} ions such as Nd^{3+} and Er^{3+} yields glasses that can be used to obtain laser amplification in the near-IR region and frequency up-conversion. On incorporation of Ln^{3+} ions into various glass matrices by conventional techniques, however, *Ln*-rich oxide clusters often form within their hosts, severely reducing the optical gain of the products. It does not seem possible to avoid clustering even with sol–gel techniques when using Ln^{3+} salts or simple homometallic alkoxides.

In search of a suitable Er-containing precursor alkoxide, different approaches can be taken. Either a homometallic alkoxide, such as the one described in this article, or a heterometallic one such as $ErAl_3(OPr^i)_{12}$ can be used (4). Erbium isopropoxide has been prepared earlier and has been described as having the formula $Er(OPr^i)_3$ (5–7). Unfortunately, no characterization useful for comparison was provided by Batwara *et al.* (5, 6), but we assume that their product is the same as that obtained by Brown and Mazdiyasni, which was characterized by FT-IR and UV–vis spectroscopy as well as mass spectroscopy (7). Its crystal structure was not determined, however. As is described in the following, the single-crystal X-ray diffraction investigations of materials giving IR and UV–vis peaks closely adhering to those reported by Mazdiyasni *et al.* revealed that the molecular formula is $Er_5O(OPr^i)_{13}$. The structure contains a square-pyramidal configuration of the Er atoms, which all are bonded to the oxo-oxygen atom situated slightly above the basal plane of the pyramid. This M_5O configuration is already known from the $M_5O(OPr^i)_{13}$ isopropoxides with M = Y (8, 9), Yb, and In (10, 11) as well as from modified alkoxides such as $Yb_5O(OMe)_8(cp)_5$ (12), $Gd_5O(OMe)_8(cp)_5$ (13), and $Ba_5OH(OCH(CF_3)_2)_9(THF)_4(H_2O)\cdot THF$ (14).

In addition to $Er_5O(OPr^i)_{13}$, another erbium isopropoxide (**I**) could be obtained by very gentle workup, i.e., only vacuum evaporation to close to dryness. Due to extensive crystal twinning, its structure could not be determined in spite of several attempts on different crystals, but properties such as solubility and stability under various conditions are reported herein.

2. EXPERIMENTAL

2.1. Equipment and Chemicals

Elemental content analyses (Er, K, Cl, and Hg) of hydrolyzed and dried samples were obtained with a scanning electron microscope (SEM, JEOL 820) equipped for energy-

[1]To whom correspondence should be addressed. E-mail: gw@inorg.su.se.

0022-4596/98 $25.00

dispersive analysis of X-ray spectra (EDS, LINK AN 10000). The presence of these elements can normally be detected down to 0.3 at.%. FT-IR spectra in the range 5000–370 cm^{-1} were recorded with a Bruker IFS-55 spectrometer from solid samples as KBr tablets and dissolved samples in a 0.1-mm path length KBr cell. UV–vis spectra in the range 200–900 nm were obtained with a Philips PU 8740 dispersive spectrometer from solutions in sealed quartz cuvettes. The behavior on heating in the range 25–225°C, obtained at a heating rate of 5°C/min, was studied with a differential scanning calorimeter (DSC, Perkin-Elmer DSC-2), using airtight steel compartments. Visual studies during heating were performed with a solid-block melting point apparatus on crystals in sealed glass capillaries. Single-crystal X-ray data were collected with a STOE four-circle diffractometer from crystals mounted in melt-sealed glass capillaries.

Preparations for syntheses and recrystallizations as well as the preparations of samples for FT-IR, UV–vis, DSC, melting point determination, and the mounting of crystals for single-crystal X-ray data collection were carried out in a glove box containing a dry, oxygen-free argon atmosphere. The reactions involving heating were performed outside the glove box in closed vessels connected to an isopiestic nitrogen atmosphere dried with P_2O_5. The oxidation was studied by adding dry oxygen with a gas-tight syringe to a double-septum-sealed flask containing the alkoxide solution. The glassware was dried at 150°C for more than 30 min before use. The toluene and 2-propanol ($HOPr^i$) solvents were dried by distillation over CaH_2. Er metal chips (Aldrich, 99.9%) and anhydrous $ErCl_3$ (Strem Chemicals, 99.9%) were used as purchased. Commercial $Al_4(OPr^i)_{12}$ (Sigma) was recrystallized before use.

2.2. *Synthesis of the Erbium Isopropoxides $Er_5O(OPr^i)_{13}$ and* **I**

Four different routes have been tried out for the synthesis of erbium isopropoxides.

Route 1: Synthesis from elemental Er. Er metal chips were (11.96 mmol, 2.000 g) added to 40 ml of a 1:1 mixture (vol:vol) of toluene and $HOPr^i$. A small amount (ca. 1 mg, 0.004 mmol) of $HgCl_2$ was added as catalyst. This mixture was heated to 75°C and left to react for 24–48 h to dissolve the metal. The resulting dark green mixture was centrifuged to give an olive precipitate and a reddish pink solution. The latter was gently evaporated to a pink, sticky mass of **I** in a yield of 40–45%.

Thorough evaporation of the sticky mass and recrystallization from toluene yielded crystals of $Er_5O(OPr^i)_{13}$ in close to quantitative yield from **I**. FT-IR and visible spectra of **I** are shown in Figs. 1 and 2, respectively. Dissolution of Er metal in 40 ml of $HOPr^i$ gave the same results as with toluene and $HOPr^i$.

Route 2A: Synthesis with $ErCl_3$ and $KOPr^i$ as starting materials. K (12.79 mmol, 0.500 g) was dissolved in 20 ml of a 1:1 (vol:vol) $HOPr^i$–toluene mixture, followed by addition of 4.263 mmol (1.176 g) of $ErCl_3$. After 2 days at room temperature, the mixture was centrifuged to separate the white precipitate formed in the reaction. The solution part was gently evaporated almost to dryness and a small amount of 2-propanol was then added. The SEM–EDS spectrum of the pink material did not show any peaks from K or Cl and IR studies showed that it was close to pure **I**. The yield was 90–95%.

Route 2B: This route is the same as route 2A, but performed at 75°C. The material obtained after gentle evaporation contained no detectable K or Cl, and the contents and yields were equal to those of route 2A.

Route 3: Metathesis with $ErCl_3$ and $KOPr^i$ and hydrolysis. K (11.0 mmol, 0.429 g) was dissolved in 16 ml of a 1:1 (vol:vol) Pr^iOH–toluene mixture, followed by dropwise addition of 0.73 ml of 1 M H_2O (0.73 mmol) in Pr^iOH–toluene 2:1 (vol:vol). One hour later, 3.655 mmol (1.000 g) of $ErCl_3$ was added and allowed to react for 2 days at room temperature, whereupon the mixture was centrifuged to separate the white precipitate formed in the reaction. On evaporation of the solvent from the solution part, crystals formed more easily than with routes 1 and 2. IR studies identified the material as pure $Er_5O(OPr^i)_{13}$, and the SEM–EDS analyses showed no contamination by K or Cl. IR and visible spectra of the compound are given in Figs. 3 and 4, respectively.

2.3. *Structure Determination of $Er_5O(OPr^i)_{13}$*

Crystals of $Er_5O(OPr^i)_{13}$ were mounted in a glass capillary (inside diameter, 1 mm) that was melt sealed in the

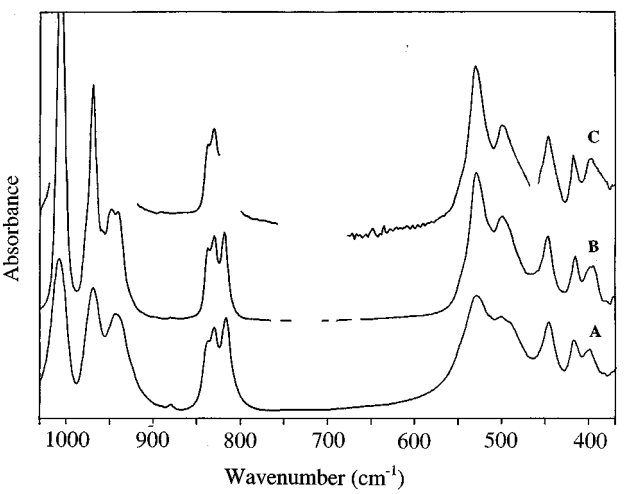

FIG. 1. FT-IR spectra of **I** as (A) solid, (B) hexane solution, and (C) toluene–2-propanol (2:1) solution.

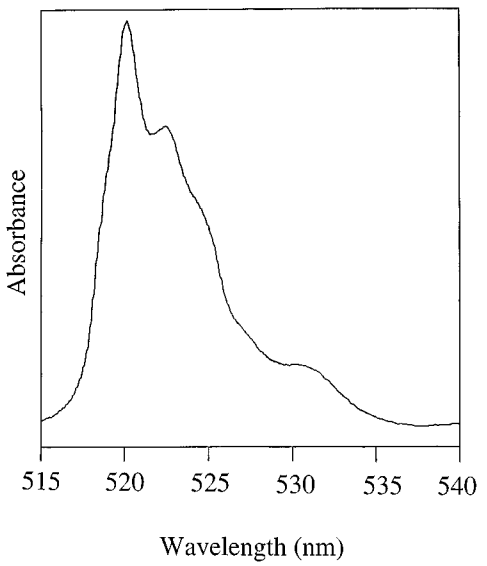

FIG. 2. Fine structure of the $^2H_{11/2} \leftarrow {}^4I_{15/2}$ transition of **I** in 2-propanol.

glove box. Single-crystal X-ray diffractometer investigation of the finally selected crystal, using Mo$K\alpha$ radiation, showed that the systematic absences in the diffraction data were consistent with the space group *Pbca* (No. 61). The unit cell parameters were determined and refined from the θ values of 50 accurately centered reflections as $a = 25.638(6)$ Å, $b = 21.575(6)$ Å, and $c = 20.917(6)$ Å. The single-crystal X-ray diffraction data were collected at $-83°$C. No correction for the absorption could be made, due to a too irregularly shaped crystal.

Preliminary Er positions were obtained by direct methods. The remaining non-hydrogen atoms were found from subsequent calculations of difference electron density ($\Delta\rho$) maps. The hydrogen atoms were positioned by assuming ideal geometry of the isopropoxo groups, and their positions were refined by constraining the carbon-to-hydrogen distance to be 1.0 Å. Due to large thermal vibrations and to the limited accuracy of the isopropoxo group geometries, the oxygen-to-carbon and carbon-to-carbon distances were restrained. In the final refinement all the metal and oxygen atoms were assumed to vibrate anisotropically, while the carbon and hydrogen atoms were held isotropic. Details of the experimental conditions and the final structural refinements are given in Table 1. Least-squares refinements of the structural model yielded an R value of 0.0748 ($R_w = 0.1158$). The final atomic coordinates with thermal parameters are given in Table 2, and selected bond distances and bond angles are listed in Table 3. The atomic scattering factors used were those for neutral atoms given in "International Tables for X-ray Crystallography" (15). The SHELXL 93 program package was used for the crystallographic calculations (16).

TABLE 1
Crystallographic Data for the Structural Investigation of $Er_5O(OPr^i)_{13}$

Formula	$Er_5O(OPr^i)_{13}$
Formula weight	1620.44 g/mol
Space group	*Pbca* (No. 61)
Unit cell dimensions	25.638(6) Å
	21.575(6) Å
	20.917(6) Å
Volume	11570(10) Å^3
Z	8
Calculated density	1.860 g cm^{-1}
μ	7.33 mm^{-1}
Temperature	$-83°$C
Weighting scheme	$1/(\sigma^2(F) + 0.001F^2)$
Final R	0.0748
Final R_w	0.1158

3. RESULTS AND DISCUSSION

3.1. The Synthesis Routes

We have tried different synthesis routes for the preparation of erbium isopropoxides: dissolution of elemental Er in 2-propanol-containing solvents (route 1) and metathetic routes involving $ErCl_3$ and $KOPr^i$ without (routes 2A and 2B) or with hydrolysis (route 3). Route 1 adhered closely to the procedure described by Brown and Mazdiyasni (7, 8), but the amount of solvent used was lower in our case. Studies of more dilute solutions gave very similar results. Metathesis specifications similar to routes 2A and 2B, using $ErCl_3$ and $NaOPr^i$, have been given by Batwara *et al.* (5). The spectroscopic characterization contained too little data from the C–O, C–C and *M*–O bands to be useful for comparison, however, which makes their results difficult to compare with ours. Route 3 involves both metathesis and hydrolysis, and this technique has not previously been reported for the preparation of *Ln* oxo alkoxides.

3.1.1. Route 1. By route 1, the only alkoxide formed was **I**, provided that the solution part was not evaporated to complete dryness. Extensive evaporation yielded increasing amounts of $Er_5O(OPr^i)_{13}$. The yield of **I** was about 40–45% from metal chips a few millimeters in size, and $HgCl_2$ catalyst was necessary for the reaction to proceed. Besides the solution of **I**, the reaction yielded a fine-grained olive-colored precipitate. This byproduct was investigated by IR spectroscopy, TGA, powder X-ray diffraction, SEM–EDS, and TEM–EDS. A detailed study of the material is in progress and will be published elsewhere, but a short description of it will be given here. The SEM–EDS study showed that the precipitate contained Er, but no Cl or Hg. The IR spectrum showed three distinct peaks, at 644, 943, and 1324 cm^{-1}, but none that could be associated with C–C, C–H or O–H groups. An IR spectrum of Er_2O_3

TABLE 2
Atomic Coordinates with Esds ($\times 10^4$) and Isotropic Thermal Parameters with Esds ($\times 10^3$) for the Erbium, Oxygen, and Carbon Atoms in $Er_5O(OPr^i)_{13}$

Atom	x	y	z	U_{eq} (Å)
		A. Erbium and Oxygen atoms		
Er1	7914(1)	3401(1)	1606(1)	50(1)
Er2	9179(1)	3144(1)	1730(1)	47(1)
Er3	9239(1)	4110(1)	2946(1)	56(1)
Er4	7977(1)	4365(1)	2824(1)	53(1)
Er5	8753(1)	4631(1)	1520(1)	49(1)
O1	8597(5)	3800(7)	2218(7)	41(4)
O2	8660(5)	3714(8)	982(7)	48(4)
O3	8426(6)	2615(7)	1692(8)	56(5)
O4	8734(6)	4983(7)	2560(7)	51(5)
O5	8882(7)	5328(9)	904(9)	78(6)
O6	7474(7)	4961(10)	3231(9)	82(6)
O7	9721(6)	2699(8)	1199(8)	67(5)
O8	7540(6)	3538(8)	2545(8)	69(6)
O9	9464(6)	3145(8)	2736(7)	56(5)
O10	9506(5)	4190(7)	1836(7)	46(4)
O11	7353(7)	3177(9)	965(9)	85(6)
O12	8549(7)	4083(10)	3557(7)	75(6)
O13	9824(8)	4495(10)	3456(9)	87(7)
O14	7868(6)	4508(7)	1722(7)	52(5)
		B. Carbon atoms		
C2	8686(9)	3675(11)	302(10)	60(7)
C2A	9193(11)	3921(14)	10(16)	102(11)
C2B	8592(12)	3021(11)	74(16)	91(10)
C3	8396(17)	1976(13)	1520(24)	177(20)
C3A	8756(17)	1553(25)	1900(26)	198(23)
C3B	7857(14)	1720(20)	1504(21)	155(17)
C4	8809(12)	5592(11)	2742(13)	83(9)
C4A	8447(13)	6036(16)	2391(15)	112(12)
C4B	8768(18)	5723(22)	3464(14)	168(19)
C5	8993(21)	5793(18)	449(21)	172(19)
C5A	9281(23)	6308(28)	766(30)	260(30)
C5B	8572(25)	6054(32)	10(35)	321(40)
C6	7162(20)	5515(20)	3315(25)	226(28)
C6A	6632(20)	5273(25)	3465(26)	204(23)
C6B	7382(22)	5874(26)	3858(28)	255(29)
C7	10150(15)	2467(22)	851(21)	174(19)
C7A	10688(20)	2338(32)	1103(28)	276(33)
C7B	10020(23)	2053(25)	300(24)	245(29)
C8	7129(14)	3183(18)	2828(19)	126(14)
C8A	7334(23)	2652(27)	3218(27)	257(29)
C8B	6552(18)	3228(37)	2852(45)	379(54)
C9	9694(14)	2690(16)	3090(16)	112(12)
C9A	9363(18)	2392(29)	3581(25)	231(27)
C9B	10251(16)	2745(34)	3220(30)	287(34)
C10	10016(9)	4339(13)	1630(14)	84(10)
C10A	10464(12)	4010(15)	1943(16)	109(12)
C10B	10097(19)	5039(14)	1774(23)	177(20)
C11	6942(14)	3103(19)	500(18)	148(16)
C11A	6474(19)	2868(24)	888(22)	204(22)
C11B	7017(21)	2662(26)	−66(22)	231(25)
C12	8465(17)	4056(20)	4230(14)	141(15)
C12A	8014(18)	3627(26)	4461(29)	224(26)
C12B	8942(20)	3813(42)	4606(45)	457(63)
C13	10197(15)	4744(20)	3852(21)	162(17)
C13A	10535(17)	4310(18)	4202(21)	160(17)
C13B	10462(25)	5348(21)	3696(33)	283(35)
C14	7486(9)	4890(12)	1414(10)	65(7)
C14A	6934(10)	4713(16)	1613(14)	98(11)
C14B	7523(12)	4876(14)	694(10)	88(9)

TABLE 3
Selected Bond Lengths (Å) with Esds for $Er_5O(OP^i)_{13}$

Er–μ_5O	Distance	Er–μ_2O	Distance
Er1–O1	2.333(13)	Er1–O3	2.151(16)
Er2–O1	2.296(13)	Er2–O3	2.245(15)
Er3–O1	2.340(13)	Er1–O8	2.206(15)
Er4–O1	2.369(13)	Er4–O8	2.187(16)
Er5–O1	2.347(14)	Er2–O9	2.227(15)
		Er3–O9	2.205(15)
Er–μ_3O	Distance	Er3–O12	2.182(16)
		Er4–O12	2.206(16)
Er1–O2	2.412(13)		
Er2–O2	2.394(13)		
Er5–O2	2.288(14)		
Er3–O4	2.422(15)	Er–μO(terminal)	Distance
Er4–O4	2.417(14)		
Er5–O4	2.305(14)	Er1–O11	2.026(16)
Er2–O10	2.416(14)	Er2–O7	2.022(13)
Er3–O10	2.426(14)	Er3–O13	2.019(15)
Er5–O10	2.253(12)	Er4–O6	2.010(16)
Er1–O14	2.403(13)	Er5–O5	2.007(16)
Er4–O14	2.344(14)		
Er4–O14	2.323(16)		

showed no peaks above 563 cm^{-1} and did not coincide at any point with that of the olive precipitate. Thermogravimetric runs in air showed that the material oxidized to form the pink Er_2O_3 at temperatures between 300 and 600°C. Assuming the final weight to be that of Er_2O_3 (382.5 g mol^{-1}), the weight at room temperature could be deduced to correspond closely to $Er_{2.0}O_{2.0}$ (366 g mol^{-1}). Powder X-ray diffraction showed that no known Er metal or Er_2O_3 form was present in the sample. With a transmission electron microscope it was confirmed that no Er metal or Er_2O_3 was present in the sample and that the crystallites were ca. 200 nm in size. The origin of the oxo atoms in the by product is intriguing, since the amount is relatively high and the amounts of water and dioxygen in the reaction mixture are very low. It seems plausible that the suboxide is formed by reduction of the 2-propanol, involving abstraction of the oxo atom to the Er metal.

3.1.2. Route 2. Synthesis of erbium isopropoxide by reaction of $ErCl_3$ with $KOPr^i$ at room temperature (route 2A) yielded a precipitate consisting almost exclusively of KCl, according to SEM–EDS analysis. The pink mass obtained by gentle evaporation of the solvent from the solution part consisted of **I** in 90–95% yield. The same synthesis done at 75°C (route 2B) gave very similar results.

3.1.3. Route 3. Synthesis, according to route 3, of erbium isopropoxide by reaction of $ErCl_3$ with $KOPr^i$, hydrolyzed with 0.2 H_2O per Er, yielded a precipitate mainly consisting of KCl according to SEM–EDS analysis. In this case, evaporation of the solution part yielded crystals more easily than routes 2A and 2B, and the compound was

identified as being pure $Er_5O(OPr^i)_{13}$. No K or Cl could be detected, and the yield was 90–95%. The easier crystallization is probably due to the fact that **I**, which is sticky when not completely dried, is not obtained in this reaction.

3.1.4. Conclusions about the synthesis routes. All three nonhydrolysis routes (routes 1, 2A, and 2B) yield **I** as the only alkoxide product in solvent mixtures from 1:1 to 1:0 $HOPr^i$–toluene. The yields obtained by dissolution of metal varied between batches but were rather low compared to the metathesis routes, which are almost quantitative. Thus, it seems that preparation of **I** is best achieved with route 2. $Er_5O(OPr^i)_{13}$ can be prepared by all routes, but routes 1 and 2 require a rather tedious vacuum decomposition of **I**. Via the hydrolysis route 3, $Er_5O(OPr^i)_{13}$ is obtained directly in very high yield, which makes it the most suitable one for the oxo isopropoxide. A solvated M_5O molecule with a trigonal-bipyramidal structure has been obtained with Nd (17), but in our studies only the non solvated $Er_5O(OPr^i)_{13}$ was formed.

3.2. *Properties of* **I**

3.2.1. Spectroscopy. An FT-IR spectrum of **I** in the range 1070–370 cm^{-1} is shown in Fig. 1. The bands below 600 cm^{-1} can be assigned to *M*–O vibrations, and those above 800 cm^{-1} to C–O and C–C vibrations. The absorptions below 1200 cm^{-1} usually show the greatest differences among alkoxides and can thus be used for identification. Peaks in this region were found for C–O and C–C at 1190 sh, 1170, 1156 sh, 1133 sh, 1127, 1078, 1008, 977 sh, 970, 945, 938 sh, 838, 830, and 817 and for *M*–O at 544 sh, 530, 500, 492 sh, 446, 416, and 399 cm^{-1}. Peaks attributable to OH stretching were found with a maximum at ca. 3190 cm^{-1}, which indicates a weak hydrogen bond. This is in accordance with the observation that the compound easily loses its solvating 2-propanol groups.

The FT-IR spectra of **I** dissolved in toluene–2-propanol (2:1) and hexane show very good resemblance to the spectrum of the solid compound, which indicates that the molecular structure is retained in solution.

The UV–vis spectrum of **I**, in 2-propanol in the range 190–900 nm showed bands typical of Er^{3+} (18). The fine structure of the peak assigned to the $^2H_{11/2} \leftarrow {}^4I_{15/2}$ transition and those due to the $^4G_{11/2} \leftarrow {}^4I_{15/2}$ and $^4F_{9/2} \leftarrow {}^4I_{15/2}$ transitions have proved useful for the identification of different heterobimetallic alkoxides (19). The fine structure of the $^2H_{11/2} \leftarrow {}^4I_{15/2}$ transition of **I** is shown in Fig. 2.

3.2.2. Solubility. The solubility of **I** is rather high in 2-propanol (up to ca. 0.8 M Er) in fresh samples, but the solubility is reduced over time, which we believe is due to loss of solvating molecules. Once these solvating groups are lost, it seems difficult to restore the compound by adding 2-propanol, although the IR spectrum is not changed much in the C–O and *M*–O regions. Likewise, **I** wetted by 2-propanol did not seem to have much greater stability than an almost dried sample. Aging also results in a formation of $Er_5O(OPr^i)_{13}$ The decomposition varied over a wide time span, ranging from full decomposition within a month to intact materials after more than a year. It seemed that larger and more well formed crystals were more stable than crystalline masses. The solubility of **I** in toluene and hexane is rather low. The higher solubility in polar solvents is contrary to that of $Er_5O(OPr^i)_{13}$, which is much more soluble in nonpolar solvents. Thus, **I** can be extracted from mixtures of **I** and $Er_5O(OPr^i)_{13}$ by dissolution in 2-propanol.

3.2.3. Stability of I toward heat, oxygen, and water. To investigate under what circumstances **I** converts to $Er_5O(OPr^i)_{13}$, we studied how its behavior was affected by heat, oxygen, and water.

Heating of solid **I** in the DSC apparatus did not give any distinct peaks, but rather several very broad ones, with some variation between different samples. This is probably due to the easy decomposition, leading to the formation of $Er_5O(OPr^i)_{13}$.

Heating a 2-propanol solution of **I** at 60°C for 7 days did not cause any degradation according to UV–vis and IR studies. This is in accordance with the fact that **I** can be formed at 75°C in routes 1 and 2B. Some solutions could be kept at room temperature for up to 6 months without decomposition, whereas others started decomposing after a few weeks. The reason for this wide span of time is not known, but it is possible that the reaction is catalyzed by some compound and that the decomposition becomes much more rapid when the first $Er_5O(OPr^i)_{13}$ is formed.

Treatment of **I** in 2-propanol, even with a large excess of dry oxygen, did not cause any decomposition for times up to 7 days at room temperature.

Hydrolysis by very slow dropwise addition to **I** in 2-propanol of 1 M H_2O in toluene–2-propanol (2:1) in the ratio 5:1 Er:H_2O produced $Er_5O(OPr^i)_{13}$ in almost stoichiometric yield.

3.2.4. Conclusions about I. The IR spectrum of the compound showed a band with peaks at ca. 3380 (weak) and 3190 cm^{-1}, which we assign to OH stretching, indicating **I** to be a solvate. Stoichiometric amounts of water added to **I** yielded $Er_5O(OPr^i)_{13}$, both in the synthesis (route 3) and directly to isolated and redissolved **I**, which indicates that it is a non-oxo isopropoxide. A solvated non-oxo isopropoxide, $Nd_4(OPr^i)_{16}(HOPr^i)_4$, has been obtained as the major product on dissolution of Nd metal in toluene-2-propanol by Helgesson *et al.* (17). It is difficult to compare the IR spectrum of the Nd compound with that of **I**, with only the peak maxima figures at hand. Dissolution of Nd metal yielded as the major component an alkoxide that showed an IR spectrum that, although showing some similarities with

I, differed enough in the band around 900 cm^{-1} for us to believe that the structures are different. The minor component in the synthesis yielded an IR spectrum very different from that of **I**. The loss of solvating molecules from **I** leads to formation of $Er_5O(OPr^i)_{13}$. A mechanism for the oxo alkoxide formation could be that the loss of solvating $HOPr^i$ molecules leads to a lowered coordination or electron donation from the ligands to the Er^{3+} ions, which might facilitate a break of a C–O bond. The oxo ions would then be able to donate more electron density and coordinate more Er^{3+} ions. Desolvation seems to be the main cause for decomposition into $Er_5O(OPr^i)_{13}$, since **I** is stable toward oxygen gas and heating in solution.

3.3. *Properties of $Er_5O(OPr^i)_{13}$*

3.3.1. Spectroscopy. An IR spectrum of the solid $Er_5O(OPr^i)_{13}$ in the range 1070–370 cm^{-1}, is shown in Fig. 3. The bands below 600 cm^{-1} are assigned to *M*–O vibrations, and those above 800 cm^{-1} to C–O and C–C vibrations. Peaks in the *M*–O and C–O vibration regions were found at 1171, 1153 sh, 1134 sh, 1125 cm^{-1}, 1119 sh, 1009, 977, 974 sh, 956 sh, 952, 839, 832, 826, 546 sh, 532, 524 sh, 502, 498 sh, 462, 448, 421 sh, 416, and 393 cm^{-1}.

The similarity of the IR spectra of $Er_5O(OPr^i)_{13}$ in the solid state and in toluene–2-propanol (2 : 1) or hexane solution shows that the molecular structure is retained in solution.

The fine structure of the $^2H_{11/2} \leftarrow {}^4I_{15/2}$ transition of $Er_5O(OPr^i)_{13}$ in toluene–2-propanol (2 : 1) is shown in Fig. 4. It is virtually unchanged in all compositions of toluene–2-propanol solvents, indicating in accordance with the IR studies that the interactions with the solvent are weak.

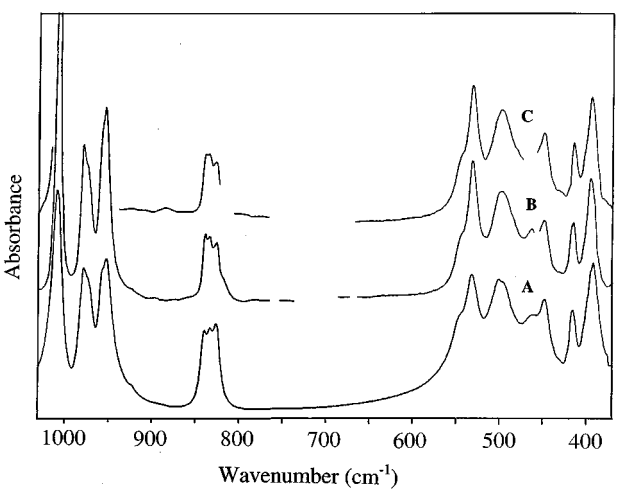

FIG. 3. FT-IR spectra of $Er_5O(OPr^i)_{13}$ as (A) solid, (B) hexane solution, and (C) toluene–2-propanol (2 : 1) solution.

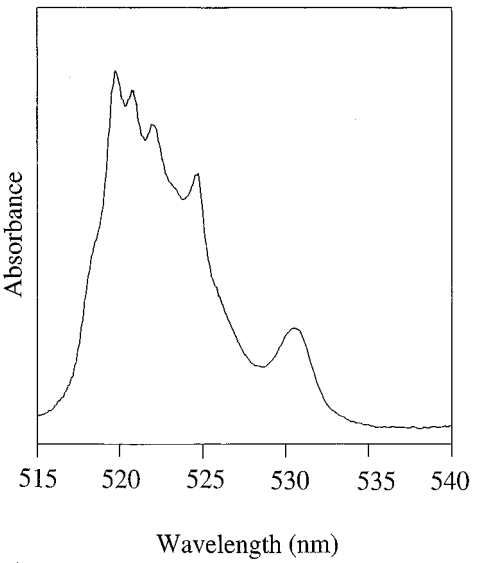

FIG. 4. Fine structure of the $^2H_{11/2} \leftarrow {}^4I_{15/2}$ transition of $Er_5O(OPr^i)_{13}$ in toluene–2-propanol (2 : 1).

3.3.2. Solubility. $Er_5O(OPr^i)_{13}$ is highly soluble in toluene (ca. 0.47 M) and hexane (ca. 0.43 M) but very sparingly soluble in 2-propanol. No aging effects on the solubility of storage in dry form have been observed.

3.3.3. Heating of solid $Er_5O(OPr^i)_{13}$. Visual inspection of crystals in melt-sealed glass capillaries showed no changes up to ca. 260°C, where the reddish pink crystals started to become slightly more matt. Thus, decomposition seems to start at ca. 260°C. The DSC curve of $Er_5O(OPr^i)_{13}$, shown in Fig. 5, has an endothermic feature with onset at 159°C and peaking at 166°C, corresponding to an energy of ca. 21 kJ mol^{-1} (curve A). This endotherm is probably due solely to melting, although melting was not visually observed in glass capillaries, since the endotherm could be

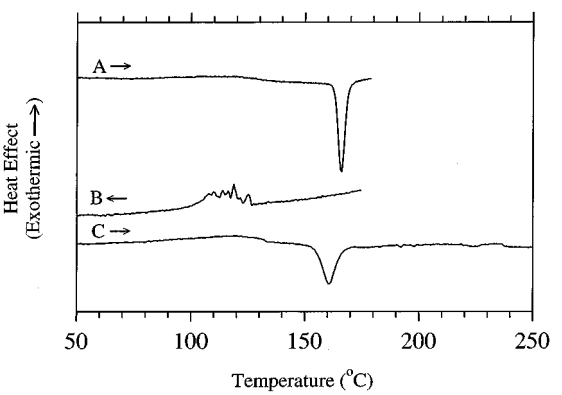

FIG. 5. DSC curve of $Er_5O(OPr^i)_{13}$ at 5°C/min obtained in a closed compartment: first run to 180°C (A), cooling from 180°C (B), and heating to 250°C (C).

reproduced after cooling from 180°C (curve C). The crystallization from the melt was observed at temperatures between 130 and 100°C (curve B). The jagged character of the cooling curve is probably due to nucleation and growth of crystallites at different temperatures. In curve C, one can also see a weak, extended exothermic peak at ca. 120–150°C. We believe that this peak corresponds to crystallization of amorphous $Er_5O(OPr^i)_{13}$, which did not have time to crystallize during cooling.

3.3.4. Reactivity of $Er_5O(OPr^i)_{13}$ toward oxygen. Addition of dry oxygen gas to $Er_5O(OPr^i)_{13}$ in toluene–2-propanol did not cause any changes for 7 days at room temperature. The compound is also stable toward decomposition at 70°C in 2-propanol–toluene for more than 7 days.

3.3.5. Reactivity of $Er_5O(OPr^i)_{13}$ with $Al_4(OPr^i)_{12}$. The $M_5O(OPr^i)_{13}$ molecule has been reported to have great stability with $M = Y$ and Nd, exemplified by $Y_5O(OPr^i)_{13}$ not reacting with $Al_4(OPr^i)_{12}$, even at elevated temperatures (9, 17). We have studied the reactivity of both $Er_5O(OPr^i)_{13}$ and $Y_5O(OPr^i)_{13}$ with $Al_4(OPr^i)_{12}$ in toluene–$HOPr^i$ 2 : 1 (vol : vol) solvent in the ratio of Er or Y to Al of 1 : 3. The analyses were made with UV–vis spectroscopy directly on the solutions for the Er compound. In this case, the fine structure of the $^2H_{11/2} \leftarrow {}^4I_{15/2}$ peak was studied. The solid Er–Al and Y–Al alkoxide mixtures formed by evaporation of the solvent after different times were studied by IR spectroscopy.

The reaction was found to be quite slow at room temperature, but much more rapid at 80°C. Most of the $Er_5O(OPr^i)_{12}$ had been consumed after less than 1 h, and the formation of $ErAl_3(OPr^i)_{12}$ (4) was complete after 2 h, according to the UV–vis spectra (see Fig. 6). Rapid evaporation of the solvent under vacuum after 2 h yielded pure $ErAl_3(OPr^i)_{12}$ according to the IR studies. Evaporation of the corresponding Y–Al mixture after 2 h yielded pure $YAl_3(OPr^i)_{12}$.

Thus, our results suggest that the reactivity of the $M_5O(OPr^i)_{13}$ square-pyramidal alkoxides is rather high, which contradicts the results obtained by other researchers who reported that $Y_5O(OPr^i)_{13}$ could be refluxed with $Al(OPr^i)_3$ without reaction, although no time was given (9). The IR spectra of the materials formed in the complete reaction of $M_5O(OPr^i)_{13}$ with $Al_4(OPr^i)_{12}$ were identical to that of $Er(Y)Al_3(OPr^i)_{12}$, whose structure has been determined (4). It has not been possible to observe where the oxo ion of the $M_5O(OPr^i)_{13}$ molecule ends up, but if it enters the $Er(Y)Al_3(OPr^i)_{12}$ molecules, the amounts of changed molecules will probably be minor. In spite of this, it should be possible to observe new peaks if the structure of the oxo alkoxide is not very similar to that of $Er(Y)Al_3(OPr^i)_{12}$. If the structures resemble each other, though, a much smaller number of isopropoxo groups will change, making observation more difficult.

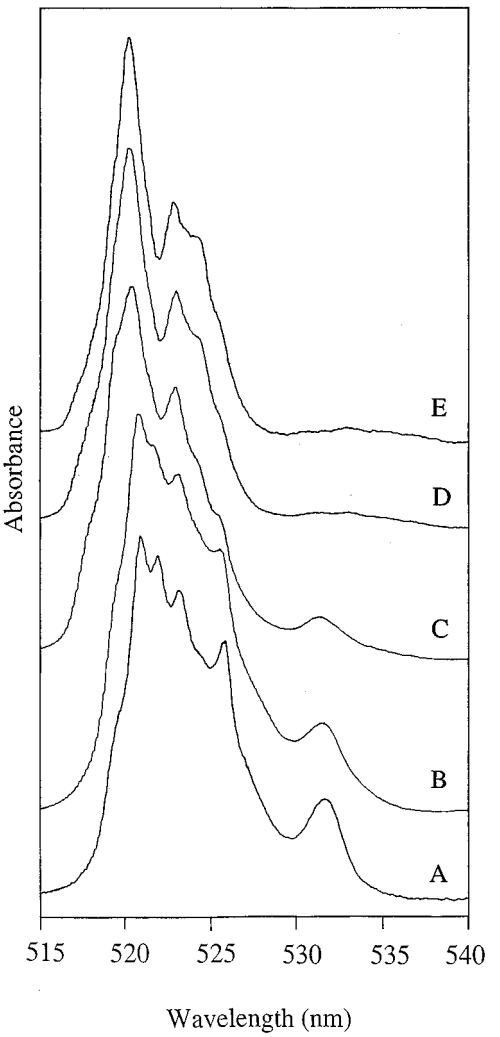

FIG. 6. Fine structure of the $^2H_{11/2} \leftarrow {}^4I_{15/2}$ peak of $Er_5O(OPr^i)_{13}$ in toluene–$HOPr^i$ (2 : 1) (A), of a mixture of $Er_5O(OPr^i)_{13}$ and $Al_4(OPr^i)_{12}$ in an Er : Al ratio of 1 : 3 in toluene–$HOPr^i$ (2 : 1) after heat treatment for (B) 0.25, (C) 1, and (D) 2 h, and of $ErAl_3(OPr^i)_{12}$ dissolved in toluene–$HOPr^i$ (2 : 1) (E).

3.4. Structure of $Er_5O(OPr^i)_{13}$

The molecular structure is shown in Fig. 7, together with the atomic labeling used for the metal and oxygen atoms.

The bond distance distribution and calculated bond valence sums (bvs values) (20) indicate that the erbium atoms are all trivalent. Each molecule consists of five erbium atoms, one oxo-oxygen atom, and thirteen isopropoxo groups, giving a molecular formula of $Er_5O(OPr^i)_{13}$. Taking the coordination around the oxygen atoms into account, the molecular formula becomes $Er_5(\mu_5\text{–}O)(\mu_3\text{–}OPr^i)_4(\mu\text{–}OPr^i)_4(OPr^i)_5$.

The Er atoms are all coordinated to the oxo-oxygen atom and to five isopropoxo groups, which gives a distorted octahedral configuration around each erbium. The

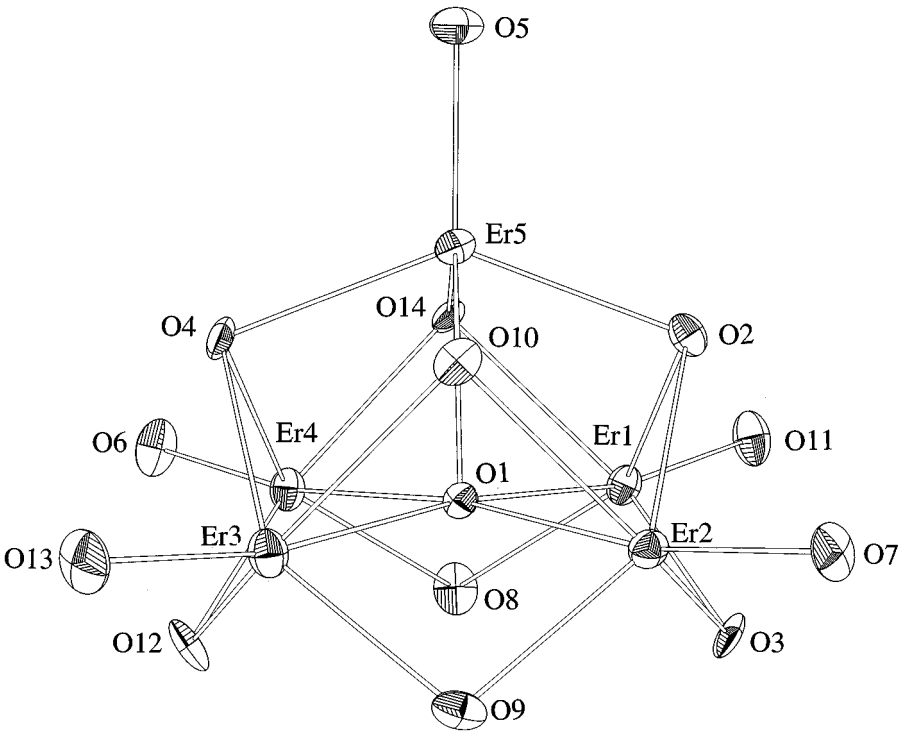

FIG. 7. ORTEP plot of the molecular structure of $Er_5O(OPr^i)_{13}$. The isopropyl groups have been left out for clarity.

molecular structure of $Er_5O(OPr^i)_{13}$ is known also for other oxo isopropoxides, such as those of Yb, Y, and In, although two different packings are observed giving an orthorhombic space group for the Er and Y compounds and a monoclinic space group for the In and Yb compounds (9–11). It also seems that, except for La, Ce, and Eu, the other lanthanide metals also yield $M_5O(OPr^i)_{13}$ when dissolved and crystallized at room temperature (21). The solvated isopropoxide $Nd_5O(OPr^i)_{13}(HOPr^i)_2$, on the other hand, which was crystallized at low temperature, has a molecular structure with a distorted trigonal-bipyramidal configuration of the M_5O group (17).

In all of the square-pyramidal M_5O structures, the oxo-oxygen atom lies above the basal plane. In the case of $Er_5O(OPr^i)_{13}$, the displacement from the basal plane is 0.162(2) Å, which is comparable to those in $Y_5O(OPr^i)_{13}$ (0.20 Å), $In_5O(OPr^i)_{13}$ (0.16 Å), and $Yb_5O(OPr^i)_{13}$ (0.19 Å).

The Er–O distances differ markedly, depending on the coordination around the oxygen atoms involved. The Er–O distances to the μ_5O-oxo-oxygen atom are rather consistent (average 2.344 Å), regardless of whether the Er atom is in the basal plane or at the top of the pyramid. The Er–μ_3O distances are shorter to the apical (average 2.287 Å) than to the basal Er atoms (average 2.400 Å). The apical erbium is coordinated to 1 oxo atom, 1 terminal isopropoxo group, and 4 μ_3-coordinated isopropoxo groups, whereas the basal Er atoms are coordinated to 1 oxo, 1 terminal isopropoxo group, and 2 μ_2- and 2 μ_3-coordinated isopropoxo groups. The shorter bond of a μ_3-coordinated isopropoxo group to an apical than to a basal Er atom is probably a result of the larger number of highly coordinated isopropoxo groups donating less electron density to the apical Er, which would render this atom more electropositive if not compensated by shorter bonds. The μ–O atoms, forming bridges between basal erbium atoms, have an average Er–O distance of 2.201 Å and a rather small variation, 2.151–2.245 Å. The terminal Er–O bonds are the shortest, with an average of 2.013 Å; these also have the largest Er–O–C angles (between 162.7° and 178.7°, average 172.5°), which might be due to multiple bonds between Er and O.

The Er–O–C angles for μ-O and μ_3-O are markedly smaller than for the terminal-O, on average 131° and 124.2°, respectively. The trends seen in $Er_5O(OPr^i)_{13}$ for Er–O bond lengths and Er–O–C bond angles are also found for the other $M_5O(OPr^i)_{13}$ compounds containing the square-pyramidal M_5O structure fragment (M = Y, Yb, and In).

4. CONCLUSIONS

Metal dissolution and metathetic routes using $ErCl_3$ and $KOPr^i$, with and without addition of water, have been investigated for the preparation of erbium isopropoxides.

Without addition of water, an erbium isopropoxide **I** was formed, which is probably a solvated non-oxo alkoxide (routes 1, 2A, and 2B). The higher yield of the metathetic routes 2A and 2B makes them the best choice for preparation of **I**. Addition of 0.2 H_2O per Er in the metathetic route (route 3) led to high-yield formation of $Er_5O(OPr^i)_{13}$. Although $Er_5O(OPr^i)_{13}$ could also be prepared by vacuum decomposition of **I**, route 3 is the most direct one and therefore the best.

The properties of **I** and $Er_5O(OPr^i)_{13}$ have been investigated. Although **I** is stable in the presence of oxygen and on heating in solution, its long-term decomposition yields $Er_5O(OPr^i)_{13}$. $Er_5O(OPr^i)_{13}$ is much more stable than **I**, and temperatures of ca. 260°C are necessary for its decomposition.

The structure of $Er_5O(OPr^i)_{13}$ was determined by single-crystal X-ray techniques to have the square-pyramidal structure known from some other M^{3+} oxo isopropoxides, e.g., $Y_5O(OPr^i)_{13}$, $Yb_5O(OPr^i)_{13}$, and $In_5O(OPr^i)_{13}$. As the molecule contains five closely connected erbium atoms and is stable in solution at room temperature toward disproportionation and reactions with alkoxides such as $Al_4(OPr^i)_{12}$, it is not suitable for sol–gel preparation of Er-doped laser amplifiers. However, heating a stoichiometric mixture of $Er_5O(OPr^i)_{13}$ and $Al_4(OPr^i)_{12}$ at 80°C yielded $ErAl_3(OPr^i)_{12}$, in which the Er^{3+} ions are isolated from each other and which is thus a good precursor.

ACKNOWLEDGMENTS

This work was supported by the Swedish National Research Council. We thank Dr. K. Jansson for making the DSC measurements. M.W. thanks the Royal Swedish Science Academy for financial support.

REFERENCES

1. C. D. Chandler, C. Rogers, and M. J. Hampden-Smith, *Chem. Rev.* **93,** 1205 (1993).
2. M. D. Shinn, W. A. Sobley, M. G. Drexhage, R. N. Brown, *Phys. Rev.* **27,** 6635 (1983).
3. Y. Nageno, H. Takebe, and K. Morinaga, *J. Am. Ceram. Soc.* **76,** 3081 (1993).
4. M. Wijk, R. Norrestam, M. Nygren, and G. Westin, *Inorg. Chem.* **35,** 1079 (1996).
5. J. M. Batwara, U. D. Tripathi, R. K. Mehrotra, and R. C. Mehrotra, *Chem. Ind.* (*London*) 1379 (1966).
6. R. C. Mehrotra and J. M. Batwara, *Inorg. Chem.* **9,** 2505 (1970).
7. K. S. Mazdiyasni, C. T. Lynch, and J. S. Smith, *Inorg. Chem.* **5,** 342 (1966).
8. L. M. Brown and K. S. Mazdiyasni, *Inorg. Chem.* **9,** 2783 (1970).
9. O. Poncelet, W. J. Sartain, L. G. Hubert-Pfalzgraf, K. Folting, and K. G. Caulton, *Inorg. Chem.* **28,** 263 (1989).
10. D. C. Bradley, H. Chudzynska, D. M. Frigo, M. E. Hammond, M. B. Hursthouse, and M. A. Mazid, *Polyhedron* **9,** 719 (1990).
11. D. C. Bradley, H. Chudzynska, D. M. Frigo, M. B. Hursthouse, and M. A. Mazid, *J. Chem. Soc., Chem. Commun.* 1258 (1988).
12. W. J. Evans, M. S. Sollberger, J. L. Shreeve, J. M. Olofson, J. H. Hain, Jr., and J. W. Ziller, *Inorg. Chem.* **31,** 2492 (1992).
13. H. Schumann, G. Kociok-Köhn, and J. Loebel, *Z. Anorg. Allg. Chem.* **581,** 61 (1990).
14. H. Vincent, F. Labrize, and L. Hubert-Pfalzgraf, *Polyhedron* **13,** 3323 (1994).
15. "International Tables for X-ray Crystallography", Vol. IV. Kynoch Press, Birmingham, 1995.
16. G. M. Sheldrick, SHELXL93, Göttingen, 1993.
17. G. Helgesson, S. Jagner, O. Poncelet, and L. G. Hubert-Pfalzgraf, *Polyhedron* **10,** 1559 (1991).
18. K. B. Yatsimirskii and N. K. Davidenko, *Coord. Rev. Chem.* **27,** 223 (1979).
19. G. Westin, R. Norrestam, M. Nygren, and M. Wijk, *J. Solid State Chem.* **135,** 149 (1998).
20. I. D. Brown and D. Altermatt, *Acta Crystallogr., Sect. B.* **41,** 244 (1985).
21. G. Westin, M. Moustiakimov, and M. Kritikos, to be published.